

## 무거운 하중 조건에서 PAO40@SiO<sub>2</sub>/UHMWPE 복합체의 마찰특성 연구

Yao Chenyu, Jia Dan, Wan Changxin, Li Jian, Zhan Shengpeng, Yang Tian,  
Qi Xiaowen\*, Liu Changxin\*, and Duan Haitao<sup>†</sup>

State Key Laboratory of Special Surface Protection Materials and Application Technology,  
Wuhan Research Institute of Materials Protection

\*School of Mechanical Engineering, Yanshan University

(2022년 4월 14일 접수, 2022년 6월 14일 수정, 2022년 7월 11일 채택)

## Tribological Properties of PAO40@SiO<sub>2</sub>/UHMWPE Composites Subjected to Heavy-loading Conditions

Yao Chenyu, Jia Dan, Wan Changxin, Li Jian, Zhan Shengpeng, Yang Tian,  
Qi Xiaowen\*, Liu Changxin\*, and Duan Haitao<sup>†</sup>

State Key Laboratory of Special Surface Protection Materials and Application Technology,  
Wuhan Research Institute of Materials Protection, Wuhan 430030, Hubei, China

\*School of Mechanical Engineering, Yanshan University, Qinhuangdao 066004, Hebei, China

(Received April 14, 2022; Revised June 14, 2022; Accepted July 11, 2022)

**Abstract:** Ultra-high molecular weight polyethylene (UHMWPE) is widely applied in heavy-loading conditions like bridge bearings, so the high hardness, high compression strength and good friction and wear properties of modified UHMWPE are needed. The PAO40@SiO<sub>2</sub> microspheres (PSM)/UHMWPE composites were prepared, and the hardness, compression strength and heavy-loading tribology properties were investigated. The result shows that the specimens with PSM have higher hardness and compression strength than pure UHMWPE. The friction coefficient and the wear rate show the tendency that decreases first and then increases with the rising of PSM content, and lower values were reached with 9 wt% PSM. PSM could improve the tribology properties by the way of both the formation of oil lubrication and the strengthen of transfer film, while the aggregation of PSM fragments would work against. The research could provide a reference for the design of self-lubricating materials under heavy load conditions such as bridge bearings.

**Keywords:** ultra-high molecular weight polyethylene, PAO40@SiO<sub>2</sub> microspheres, friction and wear, heavy-loading condition.

### Introduction

Ultra-high molecular weight polyethylene (UHMWPE) is a high-performance polymer with a set of applications. With the excellent characteristics of low coefficient of friction and high abrasion resistance, modified UHMWPE is one of the available materials for sliding sheets of bridge bearings.<sup>1-3</sup> Since the bridge bearings sliding sheets are always used under high-pressure friction caused by wind, earthquakes, the passage of vehicles, etc., the hardness and the tribology properties of sliding sheets materials under such working conditions should be

required to be superb. Generally speaking, modification is a commonly used method aiming at better mechanical and tribological properties of polymers.<sup>4-7</sup> However, the papers concentrated on friction coefficient and wear rate of modified UHMWPE with the operating conditions of high pressure only take a small percentage of the papers focusing on tribology properties of modified UHMWPE.

With the usage under high pressure, the low hardness of UHMWPE becomes a distinct disadvantage which causes excessive deformation and makes the bearing capacity decrease.<sup>8-10</sup> A general way to raise the hardness of polymers is the use of inorganic fillers, such as kaolin,<sup>11,12</sup> graphene oxide, graphite flakes,<sup>13</sup> alumina toughened zirconia,<sup>8</sup> zirconium oxide,<sup>14</sup> glass microsphere,<sup>15,16</sup> etc. So the tests of hollow

<sup>†</sup>To whom correspondence should be addressed.  
duanhaitao2007@163.com, ORCID<sup>®</sup> 0000-0002-6892-4897  
©2022 The Polymer Society of Korea. All rights reserved.

glass microsphere (HGM)/UHMWPE composites have proceeded, but the decline of friction properties occurred while the hardness of composites was raised.<sup>17</sup>

At the aim of enhancing the hardness of UHMWPE without reducing the tribological properties, lubricant materials are considered to be a well-executed secondary filler that can be used together with HGM. Since liquid lubricants have advantages like lower friction coefficient and lighter wear rate on optimizing the friction properties, it should be a great choice to introduce lubricating oil into the friction system.

But the lubricating oil is unable to be blended with UHMWPE substrate only by moulding like solid fillers because of its fluidity. Special construction is required to store the lubricating oil, and gradually release it when under a large enough pressure. Microcapsule, as is well-known, is a new type of lubricating additive with a core-shell construction, which can accommodate lubricating oil, and release it when destroyed by large pressure.<sup>18-21</sup> As such, some researchers have paid attention to polymer-based self-lubricating materials with microcapsule contained.<sup>18,22-26</sup>

In order to get the advantages of both HGM and lubricating oil, PAO40@SiO<sub>2</sub> microspheres (PSM), which mean glass microspheres filled with poly  $\alpha$ -olefin 40 (PAO40) lubricating oil, were used as the filler incorporated into the UHMWPE matrix. The hardness of PSM/UHMWPE composites was tested. The friction and wear properties of composites were investigated through a ball-on-disk friction experiment. Finally, the mechanisms of how PSM works in the process of friction were revealed. This research may provide a feasible modification scheme to enhance both the hardness and friction properties of UHMWPE under heavy load.

## Experimental

**Materials.** PSM was kindly provided by Yanshan University, the SEM image and the result of EDS analysis of which are shown in Figure 1(a). PSM consists of hollow glass microspheres and PAO40 lubricant. The proportion of PAO40 in PSM is 30 wt%, and SiO<sub>2</sub> takes the other 70 wt%. UHMWPE ( $M_w=3000000$ , mean diameter=15  $\mu\text{m}$ ) was purchased from Meideyuan Plastic Co., Ltd., Shenzhen, China, the morphology and size of which are presented by SEM image shown in Figure 1(b). The FTIR spectra of PSM, HGM (iM16K, 3m Company, USA) and UHMWPE were compared in Figure 1(c).

It could be observed from Figure 1(a) that most of the PSM

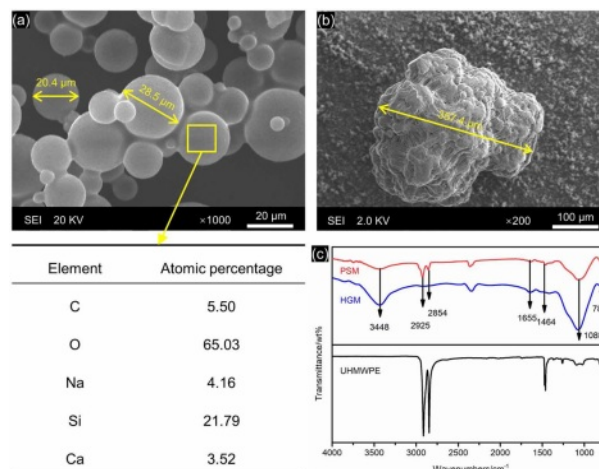


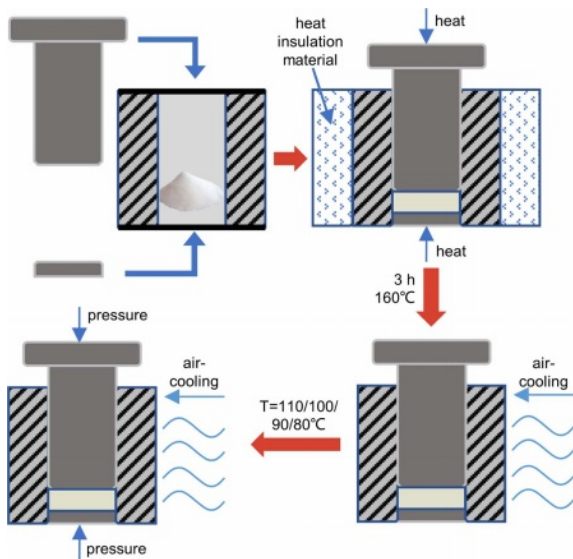
**Figure 1.** SEM image and EDS analysis of (a) PSM; (b) UHMWPE; (c) the FTIR spectra of HGM and PSM.

had a regularly spherical shape, with a diameter of about 20  $\mu\text{m}$  to 30  $\mu\text{m}$ . According to the result of EDS analysis presented in Figure 1, it is indicated that silicon took a large part among the elements, and carbon, which seems could only appear in lubricating oil, also took a proportion of elements at the outside surface of the microspheres. To analyze with FTIR images of HGM and PSM presented in Figure 1(c), peaks at 1080  $\text{cm}^{-1}$  presented on both HGM spectrum and PSM spectrum, which represents the asymmetrical stretching vibration of Si-O. And absorption peaks on PSM spectrum also occurred at 2925, 2854, and 1464  $\text{cm}^{-1}$ , which indicated the existence of the  $-\text{CH}_2$  stretching vibration and  $-\text{CH}_3$  bending vibration in PAO40 molecular,<sup>27,28</sup> and these absorption peaks don't show in the FTIR image of HGM. So it could be inferred that the PAO40 lubricating oil was wrapped in the shell of glass microspheres, and the absorption peaks belong to the residual lubricating oil on the surface of PSM during the producing process.

**Composites Preparation.** Specimens of composites consisting of different contents of PSM and UHMWPE were prepared by hot compression moulding. Powders of PSM and UHMWPE were weighted following the concentration shown in Table 1. Weighed powders were stirred for 60 min by a ball-grinding machine (F-P400H, Focucy Experimental Instruments Co., LTD, China). Mixed powders were heated to 160  $^{\circ}\text{C}$  with the moulding machine (DH-05, Donghe mechanical equipment Co., LTD, China), and a 180-min-process at 160  $^{\circ}\text{C}$  for hot compression moulding was followed, and the process of forced air cooling was followed. As the process of temperature dropping, the pressure of 10, 35, 70, and 150 MPa was respectively loaded on the mould when the temperature

**Table 1. Formula of PSM/UHMWPE Composites**  
(unit : wt%)

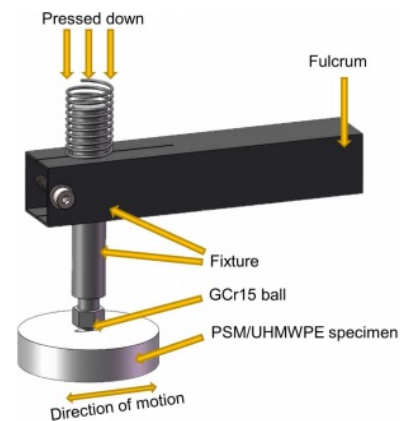
Sample No.	PSM	UHMWPE
1	0	100
2	3	97
3	6	94
4	9	91
5	12	88
6	15	85

**Figure 2.** Schematic of the molding process.

dropped to 110, 100, 90, 80 °C. The shape of the samples prepared following the above method was a disk with a diameter of 50 mm and a thickness of about 8 mm. Before further experiments, the roughness of samples was reduced to Ra 0.4 μm by sanding.

**Experiment Process.** The components of PSM, UHMWPE and composite specimens were tested by a Fourier transform infrared spectrometer (FTIR, NICOLET Is10, Thermo Fisher Scientific Inc., USA). The thermal properties of specimens were tested by a differential scanning calorimetry machine (DSC, NETZSCH DSC-204HP, Germany), the heating process of which is from the indoor temperature to 200 °C by 10 °C/min. The hardness of PSM/UHMWPE composites was measured by a Shore D hardness tester in accordance with ISO 868-2003. The compression properties of the PSM/UHMWPE composites were determined using a universal testing machine (Mester industry Ltd., China) by ISO 604:2002, for which the size of the samples were 10±0.2 mm×10±0.2 mm×10±0.2 mm.

The friction property of the specimens was characterized with ball-on-disk friction tests with a multifunctional friction and wear testing machine (MFT-5000, Rtec Instruments Inc., USA). Relative parameters are shown in Table 2. Specimens were cleaned with an alcohol solution and then dried at room temperature. As shown in Figure 3, the GCr15 ball was fixed to the fixture and pressed down against the specimen disk, and the specimen plate repeatedly moved back and forth in the horizontal direction. The distance of the reciprocating movement was 8 mm. In order to explore the friction and wear performance of the samples under heavy load conditions, it is better to let the load in experiments be higher than in working conditions. The maximum compressive stress of common bridge bearing sliding sheet products in the market is about 15 MPa to 30 MPa, and the allowable compressive stress of PTFE, the most commonly used sliding sheet material, is stipulated as 60 MPa by the European standard EN 1337-2:2004.<sup>29</sup> To create a more rigorous experimental environment, the vertical force applied on the GCr15 ball was respectively set to 50 N and 100 N, which could be converted to 82.5 MPa and 103.9 MPa for initial Hertzian contact pressure through the computation with the radius and the Poisson's ratio of contacting materials. The real-time friction coefficient was continuously stored when the reciprocating friction experiment went on. The morphology of the friction area was observed by confocal scanning optical microscope (MICRLMEASUER2,

**Figure 3.** Sketch map of ball-on-disk reciprocating friction test.**Table 2. Relative Parameters of Friction Experiments**

Material	Ball rubbing pair		Force (N)	Average sliding speed (m·s <sup>-1</sup> )	Sliding time (s)
	Diameter (mm)	Specimen disk Diameter (mm)			
GCr15	6.35	50	50	0.048	7200
			100		

Sciences et Techniques Industrielles de la Lumière, France). The wear rates of specimens were calculated with formula (1)<sup>30</sup>:

$$W = \Delta V / FL \quad (1)$$

where  $W$  is the wear rate of each specimen,  $\Delta V$  is the volume decrement,  $F$  is the normal force, and  $L$  is the total distance of the relative sliding between the ball and the disk.

In order to know further about the surface morphology and element distribution of the worn area of specimens and GCr15 balls, a JSM-6510LV scanning electron microscope (SEM, JEOL, Japan) with an EDS detector equipped was used for microscopic observation.

## Results and Discussion

**Character of Specimens.** Since the melt flow rate of UHMWPE is extremely low to about 0 g/10 min, it could be referred that PSM could only move in a small area when they were mixed with melted UHMWPE.<sup>31</sup> Therefore, the dispersity of PSM in the composite materials may almost only depends on the distribution of PSM in the mixed powder after ball-grinding. Figure 4 shows the distribution of elements C and Si on the surface of specimens. It could be observed that C and Si, which represent UHMWPE and PSM separately, are uniformly distributed.

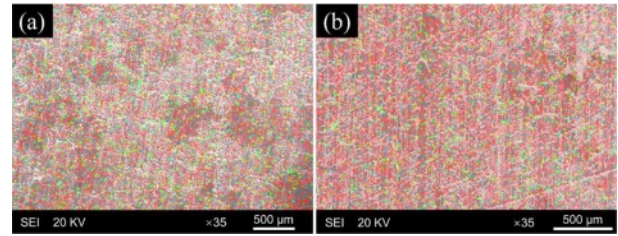


**Figure 4.** The distribution of carbon (red) and silicon (green) on the surface of (a) specimen No. 3; (b) specimen No. 4.

The surface morphology of PSM/UHMWPE composites is shown in Figure 5(a). It could be observed that PSM was successfully dispersed in UHMWPE, and a few PSM near the surface of specimens were broken or exposed on the surface of the composites because of the effect of sanding.

The FTIR spectra are shown in Figure 5(b). It is presented that the peaks placed in  $1020 \text{ cm}^{-1}$  and  $1080 \text{ cm}^{-1}$ , which indicates the existence of Si-O bonds, become stronger with large proportion of PSM. That could be evident that the ingredient which contains Si-O bonds (PSM, in other words) is equally distributed in UHMWPE matrix.

According to the previous research, the increase of crystallinity, which could be observed by a DSC test, may result in an increase of wear resistance of materials. The results of DSC tests are prepared in Figure 5(c) and (d). The composites with different proportions of PSM have similar melting points of

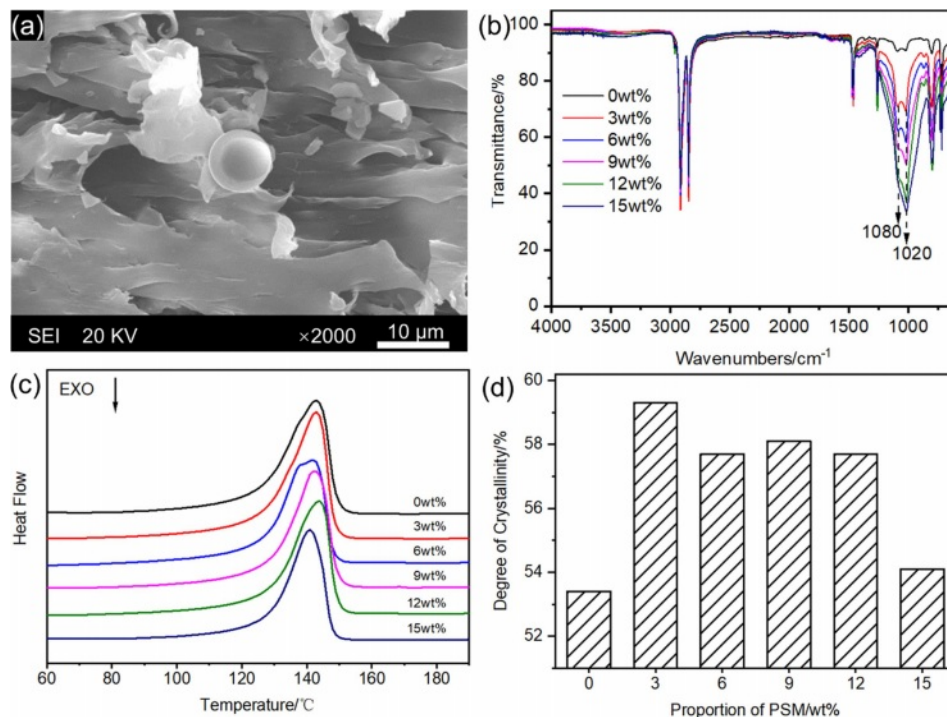


**Figure 5.** (a) SEM image; (b) FTIR spectra; (c) DSC curves; (d) crystallinity of PSM/UHMWPE composites.

nearly 140 °C, as is shown in Figure 5(c), which reveals that the introduction of PSM has less effect on the melting temperature of the UHMWPE. The specimens with proper proportions of PSM present higher crystalline than pure UHMWPE, as is shown in Figure 5(d). A possible explanation for this, is that the PSM would work as exogenous nucleating agents during the course of crystallization, which would accelerate the crystallization of UHMWPE.<sup>32</sup>

**Hardness and Compression Stress.** Hardness and compression stress are important indicators for the evaluation of the mechanical properties of materials, which show the ability of deformation resistance and failure resistance so they should be critically evaluated if the material will be used under high pressure. Hardness shows unignorable effects on tribological properties.<sup>33</sup> The hardness of PSM/UHMWPE specimens, as is shown in Figure 6, indicated a trend for rising with the increase of PSM proportion in composites. And it could be observed that the compression strength of specimens increased when the PSM were added, as is shown in Figure 7. Since PSM with glass shells could be regarded as a hard particle compared with UHMWPE, a unit amount of PSM in composites could effectively withstand a much higher load than a unit amount of UHMWPE. In another word, the adding of PSM, which has

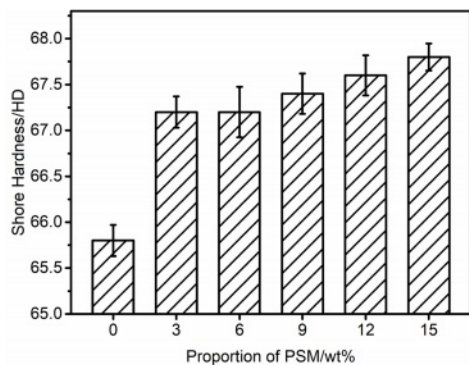


**Figure 6.** Shore hardness of PSM/UHMWPE composites.

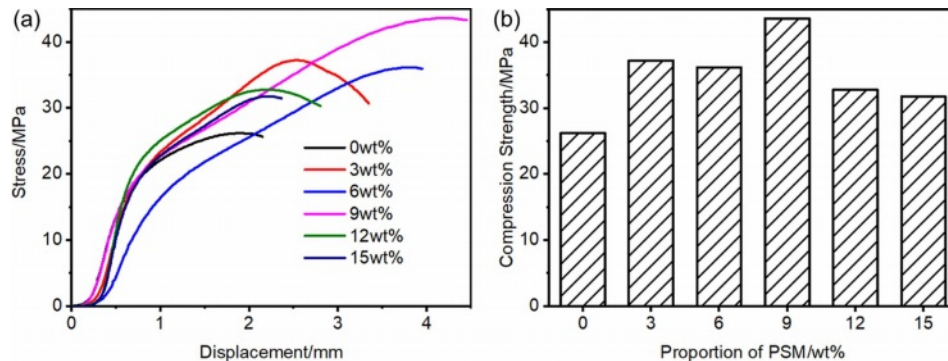


**Figure 7.** (a) Uniaxial compression stress-displacement curves; (b) the compression strength of composites with different proportion of PSM.

higher hardness than UHMWPE, could improve the deformation resistance of composites, so that the hardness and the compression strength of PSM/UHMWPE composites were obviously higher than pure UHMWPE as a result.

However, it should be noticed that the difference of hardness among the composites with PSM content between 3 to 15% was not as significant as which between pure UHMWPE and PSM/UHMWPE composites, and the compression strength of the specimens decreased when the content of PSM raised from 9 to 15 wt%. This is because the higher the amount of PSM is added, the more obvious the agglomeration of PSM will be, which will lead to the deterioration of the connection between PSM and UHMWPE, and thus hinder the increase of hardness and compression strength to a certain extent. Similar phenomena, like the agglomeration of HGM with high content of HGM in composites, were reported by some researchers.<sup>34,35</sup>

**Friction Coefficient.** Figure 8 shows the relation of the friction coefficient of composites versus time, separately under 82.5 MPa and 103.9 MPa normal loads. It is indicated that the friction coefficient of composites under 103.9 MPa normal pressure was always higher than that under 82.5 MPa normal pressure with the same PSM proportion. It could be explained according to Herzian contact theory that the radius of the contact area is proportional to the one-third power of the contact stress, and the indentation depth is proportional to the two-thirds power of the contact stress. In other words, the higher the normal pressure is, the larger the contact area is, and the deeper the indentation depth is. The expansion of the contact area and indentation depth led to the magnification of the friction coefficient.

It is presented in Figure 8 that the friction coefficient of composites with no more than 9 wt% PSM appeared an obvious rising section during the process of friction, while this section was not evident in the friction coefficient diagram of composites with more than 9 wt% PSM. Obviously, the con-

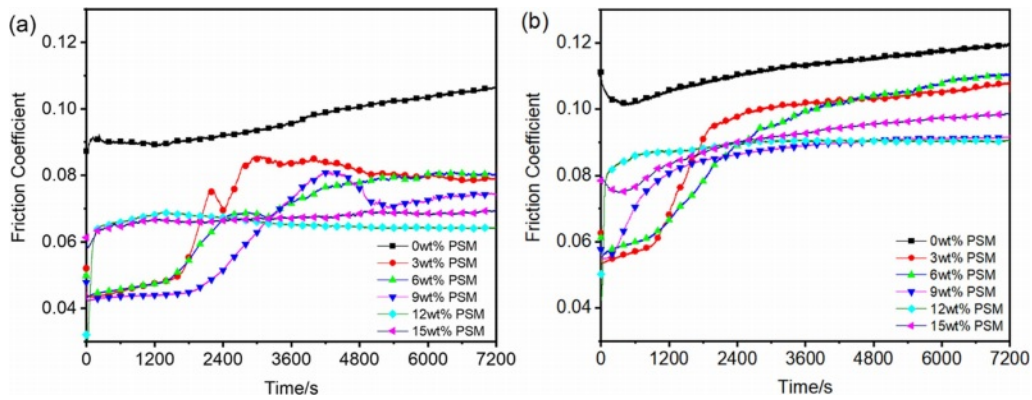


**Figure 8.** Friction coefficient of PSM/UHMWPE composites under (a) 82.5 MPa; (b) 103.9 MPa normal loads versus time.

tent of PSM showed evident effects on the friction coefficient. When composite contained less PSM, less debris working as abrasive particles might be produced by the cracking of PSM shells at the beginning section of the friction experiment, while the spilled lubricating oil worked at several areas and made the local form of friction transfer from dry friction to fluid lubricating friction. Therefore, the instantaneous friction coefficient of specimens with no more than 9 wt% PSM at the beginning of friction was much lower than that of pure UHMWPE. As time went longer, much more PSM were gradually crushed up and the number of hard debris became larger. Due to the viscosity of the lubricating oil, some of the debris aggregated with the help of oil and formed large size abrasive parts with large hardness. Such large abrasive parts weakened the antifriction effect contributed by the oil film formed by lubricating oil, so the instantaneous friction coefficient presented a large increase as the friction went on. As for specimens with more than 9 wt% PSM, large particles formed earlier because a large amount of debris was produced by the cracking of a large amount of PSM at the beginning of the friction process. Therefore, the section in which the friction coefficient largely increases appeared earlier, or even disappeared.

It is presented that the obvious rising section appeared earlier under 103.9 MPa normal pressure than under 82.5 MPa normal pressure. Obviously, the heavier the pressure was, the deeper the press-in depth of the composite specimens was. So the deformation of the specimen became larger when the initial pressure rose from 82.5 to 103.9 MPa, which led to the rupture of more PSM and accelerated the formation of aggregated large abrasive parts, which shows up as the early emergence of the obvious rising section in the figure of friction coefficient.

Figure 9 shows the average friction coefficients of composites with different proportions of PSM added. It could be

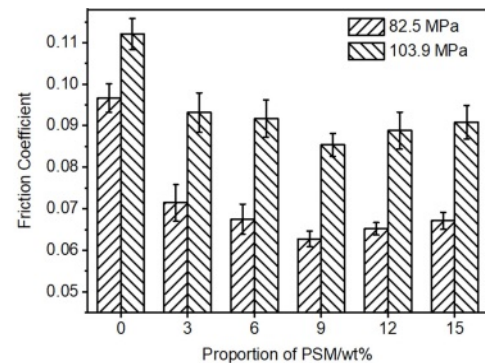


**Figure 9.** Average friction coefficient of PSM/UHMWPE composites.

observed that the average friction coefficients of specimens become lower with the rising of PSM content from 0 wt% to 9 wt%, which could be attributed to the thickening of the oil film formed by more lubricating oil spilled out from more cracked PSM. However, the trend between the average friction coefficient of composite and PSM quantity changed when the proportion of PSM became higher than 9 wt%. Specimens with 12 wt% PSM and 15 wt% PSM showed slightly higher average friction coefficients than those with 9 wt% PSM. Generally speaking, composite with 9 wt% PSM showed a lower average friction coefficient among these specimens. Respectively under 82.5 MPa and 103.9 MPa normal pressures, the average friction coefficient of PSM/UHMWPE composite with 9 wt% PSM decreased by 35.1% and 23.8% compared to that of pure UHMWPE.

**Wear Rate.** Wear rate is a vital indicator to evaluate the property of wear resistance of materials. Figure 10 shows the wear rates of the pure UHMWPE specimen and PSM/UHMWPE composite specimens. It is indicated that the wear rate of UHMWPE was decreased due to the addition of PSM. The wear rates of specimens gradually decreased when the PSM

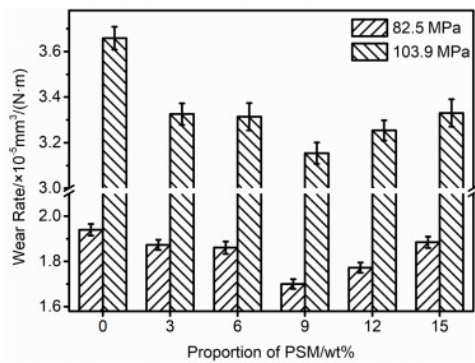


**Figure 10.** Wear rate of PSM/UHMWPE composites.

filler content increased from 0 to 9 wt% and increased when the PSM filler content increased from 9 to 15 wt%. The composite specimens with 9 wt% PSM had the minimum wear rate. The wear rate of which was 12.4% lower than pure UHMWPE under the pressure of 82.5 MPa, and 13.8% lower than pure UHMWPE under the pressure of 103.9 MPa. Additionally, it is indicated that the wear rate of specimens under 103.9 MPa vertical pressure was obviously larger than that under 82.5 MPa vertical pressure, which could be explained that the radius of the contact area and the indentation depth would become larger when vertical pressure increased based on Herzian contact theory, and the contact area was expanded, which caused the increment of wear rate.

**Wear Mechanism.** Figure 11 shows the SEM images of the worn surface morphologies of the PSM/UHMWPE composites. It shows that there were wavy traces and strip-shaped grooves parallel to the friction direction on the wear surface of pure UHMWPE specimen, which represented furrow and plastic deformation, respectively. The visibility of strip-shaped grooves began to tail off when the content of PSM was raised

to 9 wt% and reappeared when raised to 15 wt%. It also shows that the wavy traces on the specimens under 103.9 MPa vertical pressure were more obvious and more numerous than on the specimens under 82.5 MPa vertical pressure. During the friction process, lower vertical pressure means lower depth the micro-bulges pressed into the upper surface of the specimen, so that the plastic deformation with 103.9 MPa normal pressure was much more severe than with 82.5 MPa pressure.

The SEM images of the friction surfaces on GCr15 balls are shown in Figure 12, aiming in researching the condition of wear and adhesion on the rubbing pairs. It is well known that transfer films could be formed between the friction pair of pure UHMWPE and steel during the friction process. The stronger the transfer film, the better the effect of wear reduction on UHMWPE. It is displayed that the transfer film formed on the GCr15 ball rubbing with pure UHMWPE sample was in narrow strip distributions along the friction direction, while some of the composite transfer film formed on the GCr15 ball rubbing with 9 wt% PSM sample was in a plane-shaped-distributions, and the area was significantly larger than the former. With the analysis of EDS of point (e-1), (g-1), and (g-2) in Figure 12, carbon was the main content of UHMWPE transfer films, and both carbon and silicon, which represent UHMWPE and glass, respectively, were the main content of PSM/UHMWPE composite transfer films, which could confirm that the fragments of PSM shells were embedded in the transfer film during the process of friction. When PSM/UHMWPE composite specimens were heavy loaded and rubbed with GCr15 balls, lubricant in the glass microspheres appeared on the friction surface and contributed with the outstanding viscosity to the formation of UHMWPE transfer film on the surface of steel balls. Meanwhile, some glass shards came into being with

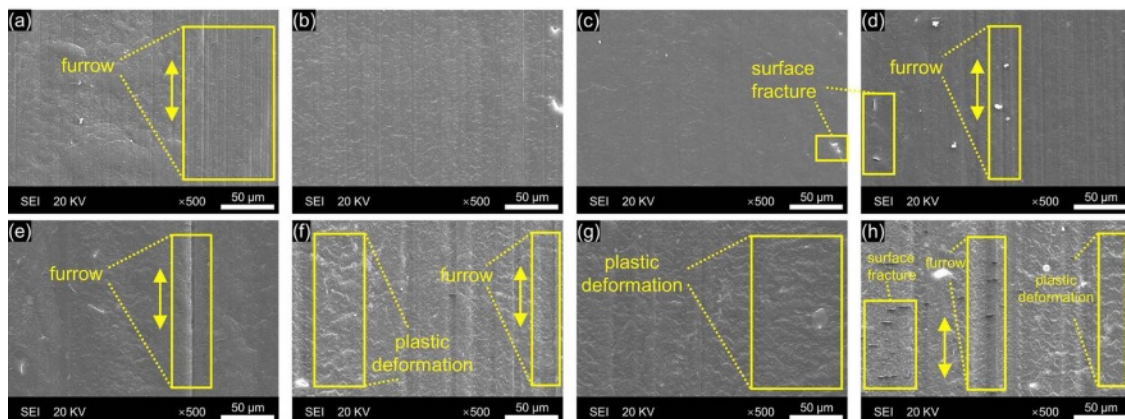


**Figure 11.** SEM images of the morphologies of the PSM/UHMWPE composites: (a), (b), (c) and (d) denote 82.5 MPa contact pressure, and PSM content of 0, 3, 9, 15 wt%, respectively; (e), (f), (g) and (h) denote 103.9 MPa contact pressure, and PSM content of 0, 3, 9, 15 wt%, respectively.

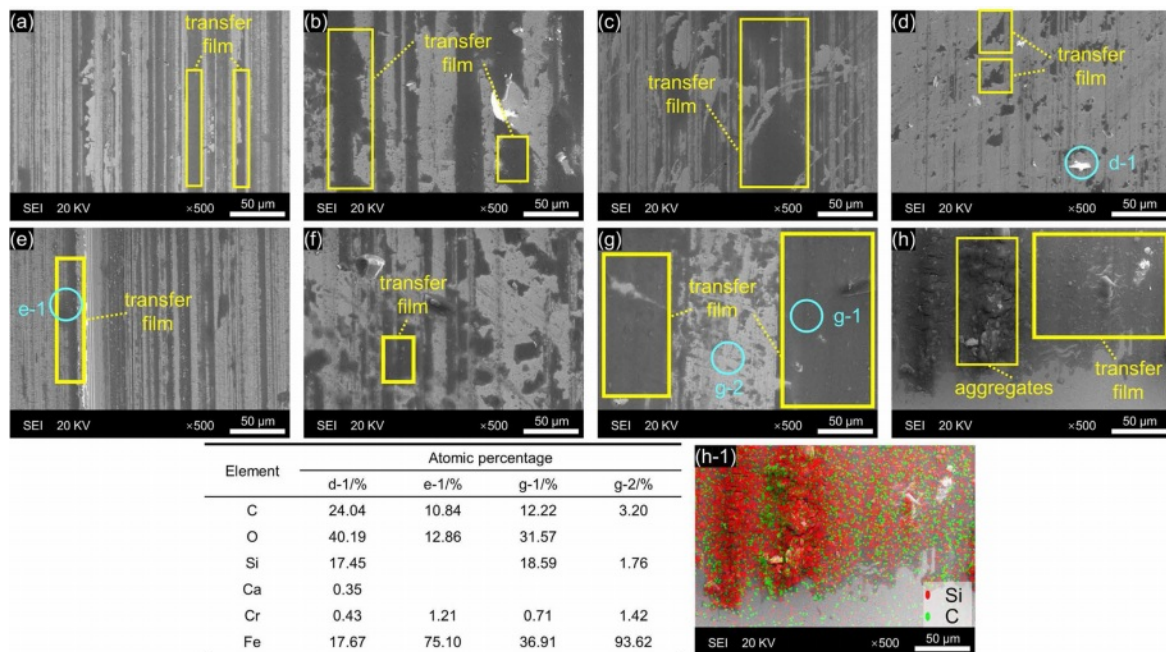


**Figure 12.** SEM images of the morphologies of the GCr15 rubbing pairs: (a), (b), (c), and (d) denote 82.5 MPa contact pressure, and PSM content of 0, 3, 9, 15 wt%, respectively; (e), (f), (g), and (h) denote 103.9 MPa contact pressure, and PSM content of 0, 3, 9, 15 wt%, respectively; (e-1), (g-1), and (g-2) show EDS analyses in spot (e-1), (g-1), and (g-2) in SEM image (e) and (g); (h-1) shows the distribution of carbon and silicon in SEM image (h).

the broken of glass microspheres, and were easily mixed in the UHMWPE transfer membrane (Figure 12(g-1)). The mechanical strength of transfer membranes was to some extent raised when glass shards were added to the list of the transfer film ingredients, and it was more difficult for the transfer film to be destroyed, reformed, and reddestroyed repeatedly during the process of friction, which could be the reason why the wear rate of the specimens decreases with the increase of PSM content. Meanwhile, the roughness of the rubbing pairs was reduced, which was conducive to achieving a good lubricating state.<sup>24</sup>

However, another factor, which is unnegligible when the PSM content was large, impeded the decrease in the wear rate of samples with the increase in PSM content. When the content of PSM in the composite material reached 15 wt%, some silicon-rich fragments and some silicon & carbon-rich particles could be observed in the SEM Figures (Figure 12(d, h)). During the friction process of PSM/UHMWPE composites, a considerable part of glass fragments generated by the cracking of the glass shell of PSM existed as abrasive particles between the friction surfaces. Cohered by lubricants, some of them were agglomerated to be large abrasive particles, which intensified the degree of abrasive wear (Figure 11(d, h)), and meanwhile caused the increasing of friction coefficient. The

distribution of transfer films on the surface of the GCr15 ball presented two situations: in some areas around the adherent aggregates, large and continuous transfer films existed; but in other areas far away from the aggregates, the transfer films were small and irregular shaped. The adhered aggregated particles worked as micro-bulges, causing the transfer film in the surrounding area to have lower pressure and be harder to fall off than in other areas. In addition, such large particles were inferred to work as abrasive particles, which could aggravate the abrasive wear by scratching out materials from the composite samples and transfer films, which led to a lower mean density of the transfer films on the GCr15 friction surface and a higher wear rate. The larger the PSM content, the stronger

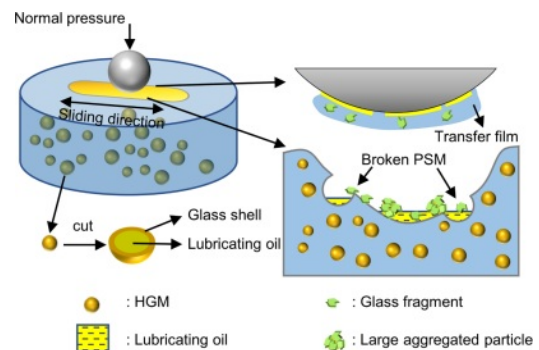


**Figure 13.** Schematic diagram of friction and wear.

the effect of large abrasive particles.

The factors which influenced the friction coefficient and wear rate could be described in Figure 13. On the one hand, the oil film formed with the oil spilled out of the crushed PSM shells, and the transfer films were strengthened with the embedded PSM fragment and the lubricating oil with high viscosity. The factors above made the tribology properties become better with the rise of PSM content from 0 to 9 wt%. But on the other hand, large aggregates could form easier with the help of the oil viscosity, which aggravated the abrasive wear.

## Conclusions

PSM/UHMWPE composites with different mass ratios were produced. Based on the application environment with heavy-load, the relation between PSM content and the hardness, and the relation between PSM content and tribology properties of composites under heavy pressure was investigated, which could be concluded as follows:

(1) UHMWPE blended with PSM had higher Shore D hardness and higher compression strength than pure UHMWPE. With the increment of PSM content, the hardness of PSM/UHMWPE composites increased less. When PSM content changed from 0 to 15 wt%, the Shore D hardness of PSM/UHMWPE rose from 65.8 to 67.8. The compression strength of composites decreased when the PSM content changed from 9 to 15 wt%, and showed a relatively high value of 43.6 MPa with 9 wt% PSM.

(2) Generally speaking, the blending of PSM could obviously improve the tribology performance of UHMWPE under the condition of heavy vertical pressure. It shows a trend that the friction coefficient and wear rate of PSM/UHMWPE composites decreased first and then increased with the increasing of PSM content, and 9 wt% is found to be the optimal PSM content for PSM/UHMWPE composites to have a better friction property.

(3) With the increment of PSM content, the oil film was thickened because more PSMs were crushed and the oil in which spilled out. Under the joint action of the bonding effect of lubricating oil and the embedding of crushed PSM shells, the transfer films were strengthened and more firmly adheres to the GCr15 ball. Meanwhile, the number of glass fragments increased, and some of them aggregated into large particles with the help of the bonding effect of oil, which aggravated the abrasive wear.

**Acknowledgment(s):** The authors would like to gratefully acknowledge the kind support of Aviation Key Laboratory of Science and Technology on Generic Technology of Self-Lubricating Spherical Plain Bearing of Yanshan University for PSM powder providing. The author(s) disclosed receipt of the following financial support for the research, authorship, and/or publication of this article: The authors thank financial support for this work from the National Natural Science Foundation of China (Grant Number: 52175183) and Project of Enterprise Technology Innovation in Wuhan (Grant Number: 2020010602012060).

**Conflict of Interest:** The authors declare that there is no conflict of interest.

## References

- Ala, N.; Power, E. H.; Azizinamini, A. Experimental Evaluation of High-Performance Sliding Surfaces for Bridge Bearings. *J. Bridge Eng.* **2016**, *21*, 04015034.
- Chang, B. P.; Akil, H. M.; Nasir, R. B. M. Comparative Study of Micro- and Nano-ZnO Reinforced UHMWPE Composites Under Dry Sliding Wear. *Wear* **2013**, *297*, 1120-1127.
- Christian, B.; Hans, S. Sliding Bearings for Civil Engineering and Material Therefor. Australian Patent 2003254542, 2003.
- Min, S. P.; Jin, K. K.; Tong-Seok, H.; Jung, T. P.; Jong, H. K. Impregnation Approach for Poly(vinylidene fluoride)/tin Oxide Nanotube Composites with High Tribological Performance. *J. Mater. Sci. Technol.* **2020**, *37*, 19-25.
- Jae, H. L.; Min, S. P.; Chang, S. L.; Tong-Seok, H.; Jong, H. K. Wear-resistant Carbon Nanorod-embedded Poly(vinylidene fluoride) Composites with Excellent Tribological Performance. *Composites Part A* **2020**, *129*, 105721.
- Han, J. T.; Wu, M. P.; Duan, W. P. GO Enhanced, Irradiation Cross-linked UHMWPE/VE Nanocomposites with Increased Hardness and Scratch Resistance. *Polym. Korea* **2020**, *44*, 589-595.
- Li, X.; Fang, S.; Yin, J.; Xu, J. Utilization of the Synergistic Effect of Talcum Powder and Bamboo Charcoal to Modify PP with Higher Dimensional Stability and Hot Deformation Temperature. *Polym. Korea* **2021**, *45*, 340-345.
- Duraccio, D.; Strongone, V.; Malucelli, G.; Auriemma, F.; De Rosa, C.; Mussano, F. D.; Genova, T.; Faga, M. G. The Role of Alumina-zirconia Loading on the Mechanical and Biological Properties of UHMWPE for Biomedical Applications. *Composites Part B: Eng.* **2019**, *164*, 800-808.
- Baena, J. C.; Peng, Z. X. Mechanical and Tribological Performance of UHMWPE Influenced by Temperature Change. *Polym. Test.* **2017**, *62*, 102-109.
- Meghashree, P.; Akshay, G.; Jayashree, B. Composites of Titanium Nano and Micro-particles and UHMWPE for Enhanced Performance Properties. *Surf. Topogr.: Metrol. Prop.* **2020**, *8*, 025013.
- Gong, G. F.; Yang, H. Y.; Fu, X. Tribological Properties of Kaolin

- Filled UHMWPE Composites in Unlubricated Sliding. *Wear* **2004**, 256, 88-94.
12. Shahzamani, M.; Rezaeian, I.; Loghmani, M. S.; Zahedi, P.; Zahedi, P. Effects of BaSO<sub>4</sub>, CaCO<sub>3</sub>, Kaolin and Quartz Fillers on Mechanical, Chemical and Morphological Properties of Cast Polyurethane. *Plast. Rubber Compos.* **2012**, 41, 263-269.
  13. Shahemi, N. H.; Liza, S.; Sawae, Y.; Morita, T.; Fukuda, K.; Yaakob, Y. The Relations Between Wear Behavior and Basic Material Properties of Graphene-based Materials Reinforced Ultrahigh Molecular Weight Polyethylene. *Polym. Adv. Technol.* **2021**, 32, 4263-4281.
  14. Kumar, S. S.; Chakravarthy, C. N.; Nithya, M. Processing and Mechanical Performances of ZrO<sub>2</sub> Reinforced Thermoplastic Nylon 6 Composites for Gear Applications. *Mater. Today: Proc.* **2021**, 37, 3038-3044.
  15. Gogoi, R.; Kumar, N.; Mireja, S.; Ravindranath, S. S.; Manik, G.; Sinha, S. Effect of Hollow Glass Microspheres on the Morphology, Rheology and Crystallinity of Short Bamboo Fiber-Reinforced Hybrid Polypropylene Composite. *JOM* **2019**, 71, 548-558.
  16. Zhang, Z. J.; Jiang, H.; Li, R.; Gao, S.; Wang, Q.; Wang, G. J.; Ouyang, X.; Wei, H. High-damping Polyurethane/Hollow Glass Microspheres Sound Insulation Materials: Preparation and Characterization. *J. Appl. Polym. Sci.* **2021**, 138.
  17. Yao, C. Y.; Yang, T.; Zhan, S. P.; Jia, D.; Li, Y. H.; Sun, Q. Y.; Li, J.; Duan, H. T. Friction and Wear Properties of Hollow Glass Microspheres/Ultrahigh Molecular Weight Polyethylene Composites Under Low Speed and High Normal Loads Conditions. *Acta. Mater. Compos. Sin.* **2022**, 39, 2623-2634.
  18. Li, X.; Ling, Y.; Zhang, G.; Yin, Y.; Dai, Y.; Zhang, C.; Luo, J. Preparation and Tribological Properties of Solid-liquid Synergetic Self-lubricating PTFE/SiO<sub>2</sub>/PAO6 Composites. *Composites Part B: Eng.* **2020**, 196, 108133.
  19. Li, X.; Wu, S.; Ling, Y.; Zhang, C.; Luo, J.; Dai, Y. Preparation and Tribological Properties of PTFE/DE/ATF6 Composites with Self-contained Solid-liquid Synergetic Lubricating Performance. *Compos. Commun.* **2020**, 22, 100513.
  20. Sun, J.; Wang, Y.; Li, N.; Tian, L. Tribological and Anticorrosion Behavior of Self-healing Coating Containing Nanocapsules. *Tribol. Int.* **2019**, 136, 332-341.
  21. Tleuova, A.; Schenderlein, M.; Mutaliyeva, B.; Aidarova, S.; Sharipova, A.; Bekturganova, N.; Miller, R.; Grigoriev, D. O. Selection and Study of Alkoxysilanes as Loading in Sub-microcapsules for Self-lubricating Coatings. *Colloids Surf. A Physicochem. Eng. Asp.* **2019**, 563, 359-369.
  22. Yan, X.; Yang, X.; Qi, X.; Lu, G.; Dong, Y.; Liu, C.; Fan, B. Tribological Properties of PAO40@SiO<sub>2</sub>/PTFE/Aramid Fabric Composites Subjected to Heavy-loading Conditions. *Tribol. Int.* **2022**, 166, 107336.
  23. Zhang, W.; Qi, X.; Li, X.; Dong, Y.; Yao, W.; Liang, L.; Zhang, Y. Surface Modification of Polysulfone/PAO40 Microcapsules via Polydopamine to Improve Thermal Stability and Used to Prepare Polyamide 6-based Self-lubricating Composite. *Colloids Surf. A Physicochem. Eng. Asp.* **2021**, 625, 126906.
  24. Zhang, L.; Xie, G. X.; Wu, S.; Peng, S. G.; Zhang, X. Q.; Guo, D.; Wen, S. Z.; Luo, J. B. Ultralow Friction Polymer Composites Incorporated with Monodispersed Oil Microcapsules. *Friction* **2021**, 9, 29-40.
  25. Yang, Z. X.; Guo, Z. W.; Yang, Z. R.; Wang, C. B.; Yuan, C. Q. Study on Tribological Properties of a Novel Composite by Filling Microcapsules into UHMWPE Matrix for Water Lubrication. *Tribol. Int.* **2021**, 153, 106629.
  26. Ma, Y.; Li, Z.; Wang, H.; Li, H. Synthesis and Optimization of Polyurethane Microcapsules Containing BMIm PF6 Ionic Liquid Lubricant. *J. Colloid Interface Sci.* **2019**, 534, 469-479.
  27. Gheisari, R.; Polycarpou, A. A. Tribological Performance of Graphite-filled Polyimide and PTFE Composites in Oil-lubricated Three-body Abrasive Conditions. *Wear* **2019**, 436, 203044.
  28. Chen, Y.; Hu, E.; Zhong, H.; Wang, J.; Subedi, A.; Hu, K.; Hu, X. Characterization and Tribological Performances of Graphene and Fluorinated Graphene Particles in PAO. *Nanomaterials* **2021**, 11, 2126.
  29. *Structural bearings. Part 2: Sliding elements*; British Standard, 2004; EN 1337-2-2004.
  30. Wan, C. X.; Yao, C. Y.; Li, J.; Duan, H. T.; Zhan, S. P.; Jia, D.; Li, Y. H.; Yang, T. Friction and Wear Behavior of Polyimide Matrix Composites Filled with Nanographite. *J. Appl. Polym. Sci.* **2022**, 139, 52058.
  31. Panin, S. V.; Buslovich, D. G.; Dontsov, Y. V.; Kornienko, L. A.; Alexenko, V. O.; Bochkareva, S. A.; Shilko, S. V. Two-Component Feedstock Based on Ultra-high Molecular Weight Polyethylene for Additive Manufacturing of Medical Products. *Adv. Ind. Eng. Polym. Res.* **2021**, 4, 235-250.
  32. Nawadon, P.; Phisut, N.; Borwon, N. Crystallization Behavior, Mechanical, Morphological and Physical Properties of Poly(butylene succinate)/Hollow Glass Microsphere Composites: Particle Size and Density Effects Observations. *J. Chem. Technol. Metall.* **2020**, 55, 324-334.
  33. Momber, A. W.; Irmer, M.; Marquardt, T. Effects of Polymer Hardness on the Abrasive Wear Resistance of Thick Organic Offshore Coatings. *Prog. Org. Coat.* **2020**, 146, 105720.
  34. Huang, C.; Huang, Z. X.; Lv, X. S.; Zhang, G. W.; Wang, Q.; Wang, B. Surface Modification of Hollow Glass Microsphere with Different Coupling Agents for Potential Applications in Phenolic Syntactic Foams. *J. Appl. Polym. Sci.* **2017**, 134, 44415.
  35. Agrawal, A.; Chandraker, S.; Sharma, A. In Physical, Mechanical and Sliding Wear Behavior of Solid Glass Microsphere Filled Epoxy Composites. *Mater. Today: Proc.* **2020**, 29, 420-426.

**Publisher's Note** The Polymer Society of Korea remains neutral with regard to jurisdictional claims in published articles and institutional affiliations.